Quantal description of nucleon exchange in a stochastic mean-field approach

S. Ayik,[1] O. Yilmaz,[2] B. Yilmaz,[3] A. S. Umar,[4] A. Gokalp,[5] G. Turan,[2] and D. Lacroix[6]
[1]*Physics Department, Tennessee Technological University, Cookeville, Tennessee 38505, USA*
[2]*Physics Department, Middle East Technical University, 06531, Ankara, Turkey*
[3]*Physics Department, Faculty of Sciences, Ankara University, 06100, Ankara, Turkey*
[4]*Department of Physics and Astronomy, Vanderbilt University, Nashville, Tennessee 37235, USA*
[5]*Department of Physics, Bilkent University, 06800, Ankara, Turkey*
[6]*Institut de Physique Nucléaire, IN2P3-CNRS, Université Paris-Sud, F-91406 Orsay Cedex, France*
(Received 21 March 2015; published 4 May 2015)

The nucleon exchange mechanism is investigated in central collisions of symmetric heavy ions in the basis of the stochastic mean-field approach. Quantal diffusion coefficients for nucleon exchange are calculated by including non-Markovian effects and shell structure. Variances of fragment mass distributions are calculated in central collisions of ^{40}Ca + ^{40}Ca, ^{48}Ca + ^{48}Ca, and ^{56}Ni + ^{56}Ni systems.

DOI: 10.1103/PhysRevC.91.054601 PACS number(s): 25.70.Hi, 21.60.Jz, 24.60.Ky

I. INTRODUCTION

The standard mean-field theory provides a good approximation for the average evolution of the nuclear collective motion at low energies, but severely underestimates the fluctuation of collective variables [1,2]. Considerable effort has been made to extend the time-dependent Hartree-Fock (TDHF) theory beyond the mean-field approximation [3–9]. The stochastic mean-field (SMF) approach goes beyond the standard mean-field description by incorporating the quantal and thermal fluctuations in the initial state [10]. The initial state fluctuations, which can be specified in a suitable manner, are incorporated into the dynamics by generating an ensemble of single-particle density matriices according to the fluctuations in the initial state. In a number of applications, it was illustrated that the SMF approach provides a very good approximation for exact quantal evolution of the many-body systems at low energies, where the collisional dissipation mechanism does not play an important role [11–13]. For a description of the approach and its various applications we refer to [14,15].

Recently, we investigated a nucleon exchange mechanism in the central [16–18] and off-central heavy-ion collisions [19] by employing the SMF approach in the semiclassical approximation and ignoring memory effect in the diffusion process. Transport coefficients extracted from the SMF approach in the semiclassical limit have a similar form as in the empirical nucleon exchange model [20], but provide a more refined description of the nucleon exchange mechanism. In the present work, we study the nucleon exchange mechanism in the fully quantal framework of the SMF approach, also incorporating the memory effect in the diffusion process, and compare the results with the semiclassical approximation. In this investigation, for simplicity, we consider the central collisions of two identical ions, i.e., symmetric collisions, at energies below the fusion barrier. In Sec. II, we present a formal description of the nucleon diffusion in the quantal framework of the SMF approach. In Sec. III, we carry out calculations of variances of fragment mass distributions in several symmetric collisions. Conclusions are given in Sec. IV.

II. QUANTAL DIFFUSION

The standard TDHF provides a deterministic description of a collision process, i.e., the system evolves from a specified initial condition to a single final state [1]. On the other hand, in the SMF approach the initial condition is specified by a distribution function characterizing the quantal and thermal fluctuations of the initial state. The initial fluctuations are incorporated into the dynamics by generating an ensemble of the single particle density matrices. The expectation values of the observables are evaluated by carrying out averages over the generated ensemble. In a single event labeled by λ, the single-particle density matrix is determined by evolving the single-particle wave functions $\Phi_j^\lambda(\vec{r},t)$ according to the self-consistent Hamiltonian in that event. Consequently, in a given event, nucleon density and current density are given by

$$\rho^\lambda(\vec{r},t) = \sum_{ij} \Phi_j^{*\lambda}(\vec{r},t)\rho_{ji}^\lambda \Phi_i^\lambda(\vec{r},t), \tag{1}$$

and

$$\vec{j}^\lambda(\vec{r},t) = \sum_{ij} \frac{\hbar}{2im}\left[\Phi_j^{*\lambda}(\vec{r},t)\vec{\nabla}\Phi_i^\lambda(\vec{r},t) - \Phi_i^\lambda(\vec{r},t)\vec{\nabla}\Phi_j^{*\lambda}(\vec{r},t)\right]\rho_{ji}^\lambda, \tag{2}$$

where labels (i,j) indicate a complete set of quantum numbers for specifying single-particle wave functions. In these expressions, elements of density matrix ρ_{ji}^λ are uncorrelated random Gaussian numbers with zero mean values $\overline{\rho_{ji}^\lambda} = 0$ and variances determined by

$$\overline{\delta\rho_{ji}^\lambda \delta\rho_{i'j'}^\lambda} = \tfrac{1}{2}\delta_{ii'}\delta_{jj'}[n_i(1-n_j) + n_j(1-n_i)]. \tag{3}$$

The average occupation numbers n_j are zero or one at zero temperature, and specified by the Fermi-Dirac distribution at finite temperatures [10]. In this expression and below, the bar over the quantities indicates the average values over the ensemble generated in the simulation. The current density for

each event obeys the continuity equation,

$$\frac{\partial}{\partial t}\rho^{\lambda}(\vec{r},t)+\vec{\nabla}\cdot\vec{j}^{\lambda}(\vec{r},t)=0. \quad (4)$$

In deep-inelastic collisions, since the binary character of the system is maintained, a set of macroscopic variables can be defined with the help of the window between the colliding ions. In the central collisions of symmetric systems, the collision geometry is rather simple, and the window is located at the origin of the center of mass frame and it is perpendicular to the collision direction. In this work, we do not differentiate between protons and neutrons, we consider only total nucleon diffusion. We can define the mass number of the projectile-like fragments in each event by integrating over the nucleon density on the right side of the window as

$$A_p^{\lambda}(t)=\int d^3r\theta(x-x_0)\rho^{\lambda}(\vec{r},t), \quad (5)$$

where $x_0=0$ denotes the location of the window, which is taken to be at the origin. According to the SMF approach, the mass number of the projectile-like fragment follows a stochastic evolution according to the Langevin equation [21,22],

$$\frac{d}{dt}A_p^{\lambda}(t)=\int dydzj_x^{\lambda}(\vec{r},t)|_{x=x_0} = v_A\left(A_p^{\lambda},t\right)+\delta v_A^{\lambda}(t), \quad (6)$$

where $j_x^{\lambda}(\vec{r},t)$ denotes component of the current density along the collision direction, which is taken to be as the x component. The fluctuations of the nucleon flux across the window in general have two contributions. One contribution arises from the event dependence of the nucleon drift coefficient $v_A(A_p^{\lambda},t)$ through the fluctuating mass number. The other part of the fluctuations arises from the elements ρ_{ji}^{λ} of the initial density matrix. In this analysis, we consider small amplitude fluctuations and ignore the event dependence of the drift coefficient. Therefore, in Eq. (6) we replace the fluctuating nucleon drift coefficient by its mean value, $v_A(A_p^{\lambda},t)\approx v_A(A_p,t)\equiv v_A(t)$,

$$v_A(t)=\frac{\hbar}{2im}\int dydz\sum_j[\Phi_j^*(\vec{r},t)\vec{\nabla}\Phi_j(\vec{r},t) - \Phi_j(\vec{r},t)\vec{\nabla}\Phi_j^*(\vec{r},t)]_{x=0}\,n_j. \quad (7)$$

The mean value of the drift is determined by the net nucleon flux across the window between colliding ions. Since in the collisions of symmetric systems, the net flux across the window is zero, the mean value of the nucleon drift vanishes, $v_A(t)=0$. The fluctuating part of the nucleon flux which arises from the initial fluctuations is given in terms of the elements ρ_{ji}^{λ} of the initial density matrix as

$$\delta v_A^{\lambda}(t)=\frac{\hbar}{2im}\int dydz\sum_{ij}[\Phi_j^*(\vec{r},t)\vec{\nabla}\Phi_i(\vec{r},t) - \Phi_i(\vec{r},t)\vec{\nabla}\Phi_j^*(\vec{r},t)]_{x=0}\,\delta\rho_{ji}^{\lambda}. \quad (8)$$

According to the Langevin description, the fluctuating flux acts as a stochastic force on the mass number. Using Eq. (3) at zero temperature, it is possible to express the correlation function of the fluctuating nucleon flux as

$$\overline{\delta v_A^{\lambda}(t)\delta v_A^{\lambda}(t')}=\sum_p G_p(t,t')+\int G_p(t,t')\rho(\varepsilon_p)d\varepsilon_p. \quad (9)$$

Here, the summation p in the first term is over the discrete negative energy particle states, while the integral in the second term is carried out over the positive energy continuum states. The density of states of the continuum states is indicated by $\rho(\varepsilon_p)$ and the quantity $G_p(t,t')$ is given by

$$G_p(t,t')=\left(\frac{\hbar}{2m}\right)^2\frac{1}{2}\sum_h[A_{ph}(t)\cdot A_{ph}^*(t') + A_{ph}^*(t)\cdot A_{ph}(t')]. \quad (10)$$

In this expression, the summation h runs over occupied hole states, and the particle-hole elements of the matrix $A(t)$ are given by

$$A_{ph}(t)=\int dydz[\Phi_p^*(\vec{r},t)\nabla_x\Phi_h(\vec{r},t) - \Phi_h(\vec{r},t)\nabla_x\Phi_p^*(\vec{r},t)]_{x=0}. \quad (11)$$

The variance of the mass distribution is defined as $\sigma_{AA}^2(t)=\overline{\delta A_P^{\lambda}(t)\delta A_P^{\lambda}(t)}$. For small amplitude fluctuations neglecting the effect arising from the fluctuations in the nucleon drift coefficient in Eq. (6), we can deduce the following equation for the variance of the fragment distribution:

$$\frac{d}{dt}\sigma_{AA}^2(t)=2D_{AA}(t). \quad (12)$$

Here, the quantal and memory dependent diffusion coefficient for nucleon exchange is determined by the correlation function of the stochastic part of the nucleon flux according to

$$D_{AA}(t)=\int_0^t dt'\overline{\delta v_A^{\lambda}(t)\delta v_A^{\lambda}(t')}. \quad (13)$$

As can be seen from Eq. (9), the nucleon diffusion coefficient is given as the sum of proton and neutron diffusion coefficients, $D_{AA}=D_{ZZ}+D_{NN}$, and there is no mixed diffusion coefficient D_{ZN} as a result of the independent nature of the nucleon exchange.

III. RESULTS

In the previous semiclassical calculations [16–19], we employed the TDHF code of Kim *et al.* with the SLy4d interaction [23]. In this work, we carry out calculations of the quantal diffusion coefficients for nucleon exchange in the central collisions of ^{40}Ca + ^{40}Ca, ^{48}Ca + ^{48}Ca, and ^{56}Ni + ^{56}Ni by employing the TDHF code of Umar *et al.* with the SLy4 interaction [24,25], and compare the quantal diffusion coefficients with their semiclassical values obtained by the code of Kim *et al.* with the SLy4 interaction. The original version of the code of Umar *et al.* calculates only the time-dependent occupied wave functions. In order to determine the quantal diffusion coefficient, we extended the code to calculate the time-dependent unoccupied single-particle wave functions in addition to the occupied hole states. In practice, 3000–4000

positive energy states have been used in calculations. The code writes the amplitudes $A_{ph}(t)$ of Eq. (11) which are calculated and stored in each time step since for calculation of Eq. (13) the entire time history is needed. This makes these calculations extremely computation intensive. Formally, the unoccupied particle states consist of a finite number of negative energy bound states and an infinite number of continuum states. In Eq. (9), we approximate the integral over the continuum states as a sum over narrow slices (bins) in the energy space as follows:

$$\int G_p(t,t')\rho(\varepsilon_p)d\varepsilon_p \approx \sum_j \overline{G}_j(t,t')\rho_j\Delta\varepsilon_j, \qquad (14)$$

where the summation run over the discrete energy bins. In this expression,

$$\overline{G}_j(t,t') = \frac{1}{N_j}\sum_{\alpha\in\Delta\varepsilon_j} G_\alpha(t,t') \qquad (15)$$

denotes the average value of the $G_\alpha(t,t')$ over the calculated states within the energy bin $\Delta\varepsilon_j$, $\rho_j = \rho(\varepsilon_j)$ is the density of states of the continuum states evaluated at the center energy ε_j of each bin, and N_j is the number of states in the interval. We use the Fermi gas expression for the density of states,

$$\rho(\varepsilon_j) = \frac{1}{2}V\left(\frac{2m}{\hbar^2}\right)^{3/2}\frac{4\pi}{(2\pi)^3}\sqrt{\varepsilon_j} = C\sqrt{\varepsilon_j}, \qquad (16)$$

where V denotes the normalization volume of the continuum states. In the calculations, we use a rectangular box of a volume $V = 24\times 24\times 49$ fm^3, which gives a value of $C = 7.0$ MeV$^{-3/2}$ for the constant C. As a technical feature, in the program there is a threshold energy for the continuum positive energy proton and neutron states, ε_p and ε_n, respectively. Since positive energy states should begin at zero value for both protons and neutrons, in the calculations we use the level density expressions with shifted energies for protons and neutrons as follows:

$$\rho_j^p = \rho_p(\varepsilon_j) = C\sqrt{\varepsilon_j - \varepsilon_p}, \qquad (17)$$

and

$$\rho_j^n = \rho_n(\varepsilon_j) = C\sqrt{\varepsilon_j - \varepsilon_n}. \qquad (18)$$

We take a uniform value $\Delta\varepsilon_j = 1.0$ MeV for the width of energy bins. The code generates a finite number of discrete continuum states. Using these continuum states and hole states we calculate the diffusion nucleon coefficient $D_{AA}(t)$, and calculate the variance of the fragment mass distribution according to

$$\sigma_{AA}^2(t) = 2\int_0^t dt' D_{AA}(t')\,. \qquad (19)$$

In principle, the variance of the fragment mass distribution should be calculated as [26]

$$\sigma_{AA}^2(t) = \sigma_{ZZ}^2(t) + \sigma_{NN}^2(t) + 2\sigma_{ZN}^2(t), \qquad (20)$$

where σ_{ZN}^2 arises from the proton-neutron correlations in the diffusion process, which is mainly driven by the symmetry energy of the binary system. In the central collisions of symmetric systems below barrier energies, because of the relatively short collision time and small energy dissipation, the correlations remain small. Therefore in the calculations, we neglect the correlations and retain only the total nucleon variance given by Eq. (19).

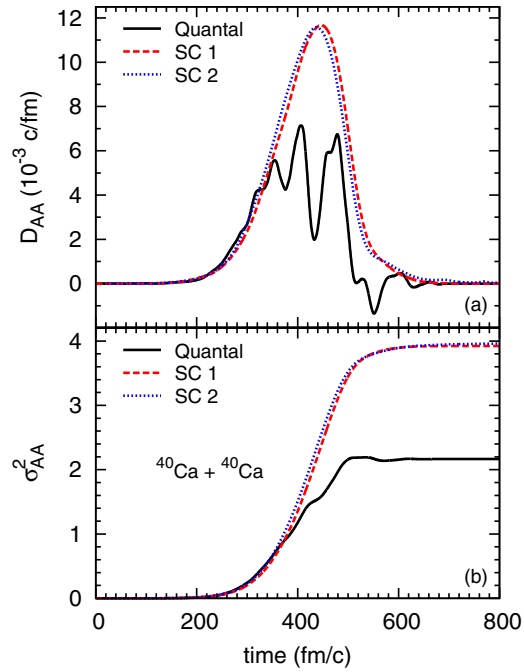

FIG. 1. (Color online) Diffusion coefficient (a) and variance of fragment mass distribution (b) as a function of time in central collision of ^{40}Ca + ^{40}Ca at 52.7 MeV. Solid, dashed, and dotted lines are the quantal and the semiclassical results with Umar *et al.*'s code and Kim *et al.*'s code, respectively.

In the calculations, we gradually increase the number of discrete continuum states until the variance of fragment mass distribution reaches approximately its saturation value. The upper panels of Figs. 1–3(a) show quantal diffusion coefficients (solid lines) for central collisions of ^{40}Ca + ^{40}Ca, ^{48}Ca + ^{48}Ca, and ^{56}Ni + ^{56}Ni at the bombarding energies, $E_{\text{c.m.}} = 52.7$ MeV, $E_{\text{c.m.}} = 50.7$ MeV, and $E_{\text{c.m.}} = 99.9$ MeV, respectively, as a function of time. The time dependence of the diffusion coefficients can also be viewed as dependence on the separation distance between ions. In the same figures, we also plot the semiclassical diffusion coefficients which are obtained with the Kim *et al.*'s code (dashed lines) and the Umar *et al.*'s code (dotted lines). The SLy4 interaction [27] is employed in both codes. The reason for using both codes is to make sure that differences between the codes do not give dissimilar results. In addition to differences in numerical procedures, Kim *et al.*'s code assumes symmetry with respect to $z = 0$ plane whereas Umar *et al.*'s code does not. Furthermore Umar *et al.*'s code contains few extra time-odd terms for the Skyrme interaction [24]. As we see the results from the two codes are in a reasonable agreement. Diffusion calculations are carried out at bombarding energies slightly below the barriers. Consequently collisions do not lead to fusion in the mean-field description, after touching, the colliding ions exchange

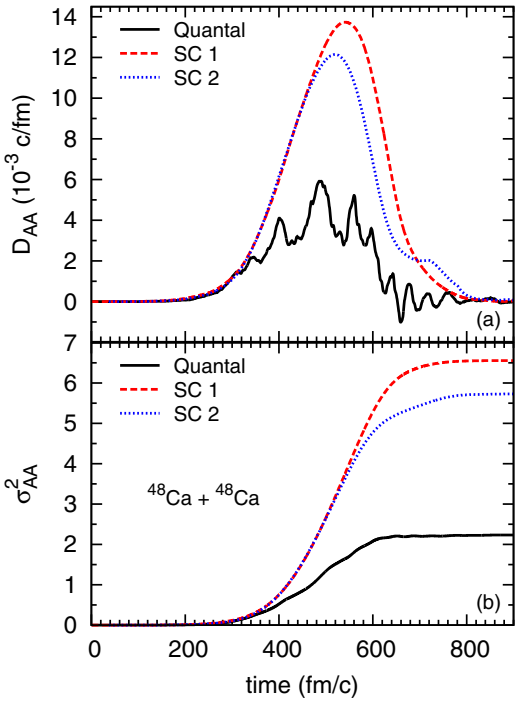

FIG. 2. (Color online) Diffusion coefficient (a) and variance of fragment mass distribution (b) as a function of time in central collision of ^{48}Ca + ^{48}Ca at 50.7 MeV. Solid, dashed, and dotted lines are the quantal and the semiclassical results with Umar *et al.*'s code and Kim *et al.*'s code, respectively.

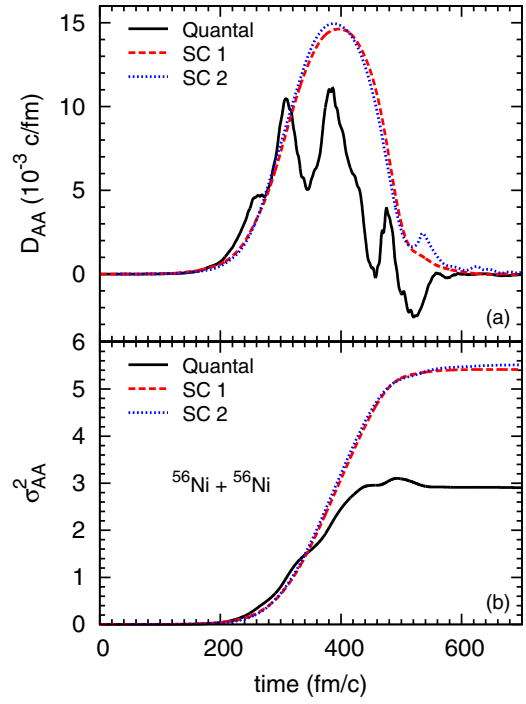

FIG. 3. (Color online) Diffusion coefficient (a) and variance of fragment mass distribution (b) as a function of time in central collision of ^{56}Ni + ^{56}Ni at 99.9 MeV. Solid, dashed, and dotted lines are the quantal and the semiclassical results with Umar *et al.*'s code and Kim *et al.*'s code, respectively.

several nucleons and reseparate again. Overall magnitudes of the quantal diffusion coefficients are smaller than their semiclassical values and exhibit oscillations as a function of time. These oscillations in quantal calculations are partly due to the shell structure of the nuclei and partly due to the memory effect. In fact, as a result of the non-Markovian behavior, diffusion coefficients take negative values during the separation stage of the collision. On the other hand, the semiclassical calculations exhibit a smooth behavior as a function of time or the separation distance. Part (b) in Figs. 1–3 shows the variances of the fragment mass distributions for the same systems at the same energies. The solid lines indicate the quantal results, while and the result of semiclassical calculations obtained in Kim *et al.*'s code and Umar *et al.*'s code are shown by dashed and dotted lines, respectively. The variances of the fragment mass distributions calculated in the semiclassical approximation by employing two different TDHF codes are in relatively good agreement with each other. On the other hand, the magnitude of quantal variances is smaller than the semiclassical results by nearly a factor of two in collisions of ^{40}Ca + ^{40}Ca and ^{56}Ni + ^{56}Ni, and a factor of three in ^{48}Ca + ^{48}Ca. This difference between the quantal and the semiclassical calculations are partly due to genuine quantal effects, shell structure and non-Markovian behavior in the diffusion coefficients. On the other hand, an important part of the difference between the quantal and the semiclassical results may be due to the density of states factor of the continuum states. In the calculations we employ the Fermi gas level density expression, which underestimates the actual density of the positive energy continuum states.

IV. CONCLUSIONS

In this work, we investigate the nucleon exchange mechanism in the quantal framework of the SMF approach. We carry out calculations of nucleon diffusion coefficients and variances of fragment mass distributions for central collisions of ^{40}Ca + ^{40}Ca, ^{48}Ca + ^{48}Ca, and ^{56}Ni + ^{56}Ni at the bombarding energies, $E_{\text{c.m.}} = 52.7$ MeV, $E_{\text{c.m.}} = 50.7$ MeV, and $E_{\text{c.m.}} = 99.9$ MeV, respectively. These bombarding energies are slightly below the fusion barriers of these systems. Consequently, colliding ions in the TDHF description do not fuse, but during contact they exchange several nucleons and separate again. In the quantal calculations we employ the TDHF code of Umar [24,25], which is extended for obtaining time-dependent particle states. We compare the quantal diffusion coefficients and the quantal variances of the fragment mass distributions with those obtained in the semiclassical framework by employing the TDHF code of Umar *et al.* and also the TDHF code of Kim *et al.* The quantal variances are smaller than those obtained in the semiclassical approximation by nearly a factor of two in collisions of ^{40}Ca + ^{40}Ca and ^{56}Ni + ^{56}Ni, and a factor of three in ^{48}Ca + ^{48}Ca. The difference in the results partly arises from the shell structure and non-Markovian effects in the quantal calculations. In the quantal calculations of diffusion

coefficients, we use the Fermi gas expression for the level density of positive energy continuum sates. An important part in the difference between quantal and semiclassical result may be due to the Fermi gas expression, which underestimates the actual level density continuum states. Further studies are needed to clarify the effect of the level density of continuum states on the quantal diffusion coefficients of nucleon exchange in heavy-ion collisions.

ACKNOWLEDGMENTS

S.A. and S.U. gratefully acknowledge TUBITAK and Middle East Technical University for partial support and warm hospitality extended to them during their visits. This work is supported in part by US DOE Grants No. DE-FG05-89ER40530 and No. DE-FG02-96ER40975, and in part by TUBITAK Grant No. 113F061.

[1] C. Simenel, Eur. Phys. J. A **48**, 152 (2012).
[2] J. W. Negele, Rev. Mod. Phys. **54**, 913 (1982).
[3] R. Balian and M. Veneroni, Phys. Lett. B **136**, 301 (1984).
[4] S. Ayik and C. Gregoire, Phys. Lett. B **212**, 269 (1988); Nucl. Phys. A **513**, 187 (1990).
[5] J. Randrup and B. Remaud, Nucl. Phys. A **514**, 339 (1990).
[6] Y. Abe, S. Ayik, P.-G. Reinhard, and E. Suraud, Phys. Rep. **275**, 49 (1996).
[7] D. Lacroix, S. Ayik, and Ph. Chomaz, Prog. Part. Nucl. Phys. **52**, 497 (2004).
[8] C. Simenel, B. Avez, and D. Lacroix, *Quantum Many-Body Dynamics: Applications to Nuclear Reactions* (VDM Verlag, Germany, 2010).
[9] M. Tohyama and A. S. Umar, Phys. Lett. B **549**, 72 (2002).
[10] S. Ayik, Phys. Lett. B **658**, 174 (2008).
[11] D. Lacroix, S. Ayik, and B. Yilmaz, Phys. Rev. C **85**, 041602(R) (2012).
[12] D. Lacroix, D. Gambacurta, and S. Ayik, Phys. Rev. C **87**, 061302(R) (2013).
[13] B. Yilmaz, D. Lacroix, and R. Curebal, Phys. Rev. C **90**, 054617 (2014).
[14] D. Lacroix and S. Ayik, Eur. Phys. J. A **50**, 95 (2014).
[15] O. Yilmaz, S. Ayik, F. Acar, and A. Gokalp, Phys. Rev. C **91**, 014605 (2015).
[16] S. Ayik, K. Washiyama, and D. Lacroix, Phys. Rev. C **79**, 054606 (2009).
[17] K.Washiyama, S. Ayik, and D. Lacroix, Phys. Rev. C **80**, 031602(R) (2009).
[18] B. Yilmaz, S. Ayik, D. Lacroix, and K. Washiyama, Phys. Rev. C **83**, 064615 (2011).
[19] J. Randrup, Nucl. Phys. A **307**, 319 (1978); **327**, 490 (1979); **383**, 468 (1982).
[20] B. Yilmaz, S. Ayik, D. Lacroix, and O. Yilmaz, Phys. Rev. C **90**, 024613 (2014).
[21] C. W. Gardiner, *Quantum Noise* (Springer, Berlin, 1991).
[22] U. Weiss, *Quantum Dissipative Systems* (World Scientific, Singapore, 1999).
[23] K.-H. Kim, T. Otsuka, and P. Bonche, J. Phys. G **23**, 1267 (1997).
[24] A. S. Umar and V. E. Oberacker, Phys. Rev. C **73**, 054607 (2006).
[25] A. S. Umar, M. R. Strayer, J.-S. Wu, D. J. Dean, and M. C. Güçlü, Phys. Rev. C **44**, 2512 (1991).
[26] W. U. Schroder, J. R. Huizenga, and J. Randrup, Phys. Lett. B **98**, 355 (1981).
[27] E. Chabanat, P. Bonche, P. Haensel, J. Meyer, and R. Schaeffer, Nucl. Phys. A **635**, 231 (1998).